Macromolecules
ARTICLE

Macromolecules **2010**, *43*, 9821–9827 **9821**
DOI: 10.1021/ma102117f

Anisotropy of the Segment Mobility versus Self- and Pair-Correlation Functions in Polymer Melts under Mesoscopic Confinement

Rainer Kimmich*,† and Nail Fatkullin‡

†*Universität Ulm, 89069 Ulm, Germany, and* ‡*Department of Physics, Kazan Federal University (former Kazan State University), Kazan 420008, Tatarstan, Russia*

Received September 14, 2010; Revised Manuscript Received November 4, 2010

ABSTRACT: Techniques typically used for studies of polymer dynamics such as NMR relaxometry, quasielastic neutron scattering, multiple-quantum build-up NMR, dielectric relaxation spectroscopy, and mechanical relaxation are specified and commonly classified in terms of correlation functions. Two categories of correlation functions are identified with respect to their specific ability to describe translational fluctuations on the one hand, and molecular reorientations on the other. The first category is of the dynamic-structure factor type reflecting the absolute or relative displacement behavior of particles. This type of function is in contrast to the second category, namely correlation functions of spherical harmonics of different orders characterizing rotational diffusion of molecules or molecular groups. In polymers, rotational diffusion tends to be strongly anisotropic. It is elucidated that the long-time tail of the correlation decay is particularly indicative for model characteristic features. The representation of experimental results by correlation functions instead of method-specific technical terms permits unambiguous comparisons and interpretations based on different techniques. This is demonstrated in the context of a problem of particularly topical interest, namely polymer melts confined in nanoscopic porous matrices. Methods probing correlation functions of spherical harmonics are shown to be sensitive to rotational chain dynamics severely modified under geometrical confinement, the so-called corset effect. On the other hand, correlation functions of the dynamical structure factor type characterizing translational fluctuations reveal little influence of such constraints in the experimentally accessible time/space window. In order to support this classification, the potentially competitive influence of wall adsorption effects is discussed in addition. Criteria permitting to rule out this sort of retardation mechanism under appropriate conditions are specified.

Introduction

The purpose of this article is to elucidate effects on chain dynamics in polymer melts due to confinement in nanometric porous matrices. This in particular refers to finite-size phenomena on a purely geometric basis to be distinguished from adsorption at walls of the confining matrices. Because of their obvious relevance for surface coating, lubrication and other (nano)technological applications, properties of the latter class of confined systems have been examined extensively in the literature.[1,2] In contrast to those studies, the focus of the present paper will be on systems where wall adsorption has no or only negligible influence on polymer chain dynamics.[2] In most confinement scenarios of practical significance, i.e. thin polymer films,[3] polymers in porous media,[4−7] polymer emulsions,[8] polymer composite systems,[9] agglomerates of polymers with filler particles, etc., both adsorption and finiteness of the polymer phases may play a role at the same time for chain dynamics. For theoretical treatments and model descriptions of confined-chain dynamics, it is therefore most important to analyze the origins of the confinement effects. We will restrict ourselves to systems where this distinction is feasible, and where the dominant contribution of finite-size restrictions of molecular motions is evident.

Concomitant to the developments of mesoscopic technologies in the past one or two decades, much attention has been paid to all phenomena relevant for the submicrometer length scale. In this sense, finite-size effects may be of interest per se. It should however be emphasized that all dynamic features specific for polymers under confinement will be decisive for our understanding of chain dynamics under bulk conditions: Bulk phases are the limiting cases of less and less restricted polymers under confinement. This can be exemplified with the fluctuating free volume, the anisotropy of segment mobility, and correlations of modes of neighboring chains.

In the following, different experimental techniques for the investigation of polymer dynamics will be considered and compared. As a classification, we distinguish methods sensitive to orientation correlation functions from those probing translational particle displacements.

Rotational and translational fluctuations are best described with the aid of correlation functions of the type

$$G(t) = \langle A(t) \cdot B^*(0) \rangle \tag{1}$$

where $A(t)$ and $B(t)$ are orientation or position dependent functions of time. These functions are usually complex (see the examples below and ref 10), and B^* is conjugate complex to B. The triangular brackets indicate an ensemble average. The orientation of a molecule can be specified by the polar and azimuthal angles $\vartheta(t)$ and $\varphi(t)$, respectively, spanned by a molecular axis relative to the laboratory frame the z axis of which in turn is established by an external field (e.g., a magnetic flux density). In terms of spherical harmonics, the "orientation correlation function" characterizing rotational fluctuations is defined by

$$G_r^{l,m}(t) = \langle Y_{l,m}(t) Y_{l,-m}(0) \rangle \tag{2}$$

where the spherical harmonics are sine and cosine terms of $\vartheta(t)$ and $\varphi(t)$. Typical methods probing this sort of correlation function are field-cycling NMR relaxometry ($l = 2$, $m = 1,2$),[11] transverse

*Corresponding author.

Published on Web 11/15/2010

relaxation ($l = 2, m = 0,1,2$),[12] multiple-quantum build-up NMR ($l = 2, m = 0$),[8] and dielectric relaxation ($l = 1, m = 0$).[13,14] The detailed conditions under which the specified orders of the spherical harmonics and the "single-particle" character of the correlation functions eq 2 are valid will be discussed below.

Translational fluctuations can be described by the "self-correlation function"

$$G_t^{self}(t) = \langle \mathrm{e}^{-i\mathbf{k}\cdot\mathbf{R}(0)} e^{i\mathbf{k}\cdot\mathbf{R}(t)} \rangle \underset{\text{Gaussian propagator}}{\approx} \exp\left\{ -\frac{1}{6} k^2 \langle \Delta R_{self}{}^2 \rangle \right\} \tag{3}$$

where $\boldsymbol{R}(0)$ and $\boldsymbol{R}(t)$ are the position vectors of a particle at times 0 and t, respectively. $\boldsymbol{k}$ is a wave vector specifically defined for the method under consideration. In the literature the propagator of the diffusion process is often assumed to be a Gaussian function. In this case, the correlation function can be expressed in terms of the mean square displacement $\langle \Delta R_{self}{}^2 \rangle = 6Dt$, i.e. the second moment of the propagator. Note, however, that with polymers the Gaussian assumption can only be taken as a very crude approach (see below). Well-known techniques probing this correlation function are field-gradient NMR diffusometry in its different variants[15] and incoherent (quasielastic) neutron scattering[17] (compare ref 16). The latter phenomenon dominates for protons which possess a particularly strong incoherent scattering cross section. In the context with scattering experiments, eq 3 is usually called "incoherent dynamic structure factor" or "incoherent scattering function".

Translational displacements of particles relative to each other are described by the "pair correlation function"

$$\begin{aligned} G_t^{pair}(t) &= \frac{1}{n} \sum_{j,l=1}^{n} \langle \mathrm{e}^{-i\mathbf{k}\cdot\mathbf{R}_j(0)} e^{i\mathbf{k}\cdot\mathbf{R}_l(t)} \rangle \\ &= \frac{1}{n} \sum_{j,l=1}^{n} \langle \mathrm{e}^{-i\mathbf{k}\cdot(\mathbf{R}_j(0)-\mathbf{R}_l(t))} \rangle \\ &= \frac{1}{n} \sum_{j,l=1}^{n} \langle \mathrm{e}^{-i\mathbf{k}\cdot\Delta\mathbf{R}_{j,l}(t)} \rangle \end{aligned} \tag{4}$$

referring to particle pairs j,l. These particles can be located on the same or on different molecules depending on the system under investigation. That is, one can distinguish intra- and intermolecular pair correlation functions. In the latter case and if the molecules diffuse independently of each other, a Gaussian propagator of the relative displacements, $\Delta\boldsymbol{R}_{j,l}(t)$, can be assumed so that the intermolecular pair correlation function can be approached by

$$G_t^{pair}(t) \underset{\text{Gaussian propagator}}{\approx} \frac{1}{n} \sum_{j,l=1}^{n} \exp\left\{ -\frac{1}{6} k^2 \langle \Delta R_{j,l}{}^2(t) \rangle \right\} \tag{5}$$

The information inherent to the intermolecular pair correlation function can be examined with the aid of isotopic dilution NMR relaxometry, that is by typically studying proton NMR in partially deuterated samples. In principle, the intramolecular variant can also be studied on this basis by referring to the residual protons of perdeuterated molecules.[18] More frequently and successfully, however, the intramolecular pair correlation function is acquired with the aid of coherent (quasielastic) neutron scattering.[17] Owing to the fact that the coherent scattering cross section of deuterons is significantly stronger than that of their incoherent contribution, coherent neutron scattering can be identified with the aid of deuterons as scattering centers in isolated perdeuterated species. In this context, eq 4 is also called "coherent dynamic structure factor" or "coherent scattering function".

Unlike simple, low-molecular liquids, correlation functions characterizing molecular dynamics in complex systems tend to be intrinsically nonexponential. It is therefore most important to probe these functions in a range as wide as technically possible. Moreover, there is some tendency that short-time (i.e., short-range) fluctuations dominate most of the correlation decay whereas the system-specific (i.e., long-range) part of the information is contained in a small, slowly decaying tail comprising only a few percent of the total correlation loss. Since one is usually interested in features specific for the system, a corresponding measuring capability should be ensured. This, in particular, means a sensitive time window to acquire the long-time tail and a detection sensitivity permitting the record of a few percent residual correlation or less.

Short-time dynamics of polymer chains is governed by short-range modes. On the other hand, only long-range modes can be expected to be sensitive to confinement effects. That is, only techniques sensitive to long times and correspondingly small residual correlations are suitable for corresponding investigations. We will therefore restrict the discussion to experiments complying with this condition.

In the following we will particularly refer to field-cycling NMR relaxometry, a technique probing rotational fluctuations via the spin−lattice relaxation time T_1 in a wide frequency range (or in Fourier conjugate form in a wide time range). In cases where intramolecular dipolar or quadrupolar spin interactions dominate, the spin−lattice relaxation rate as the inverse spin−lattice relaxation time can be approached by

$$\begin{aligned} \frac{1}{T_1} &\approx C \int_{-\infty}^{\infty} G_r^{2,1}(t) \mathrm{e}^{-i\omega t}\, \mathrm{d}t \equiv C\mathcal{F}\{G_r^{2,1}(t)\} \\ &\equiv C\mathcal{F}\{\langle Y_{2,1}(t)\, Y_{2,-1}(0)\rangle\} \end{aligned} \tag{6}$$

It obviously reflects the Fourier transform $\mathcal{F}\{...\}$ of the orientation correlation function eq 2 for $l = 2$, $m = 1$.[2] The spherical harmonics in eq 6 is defined by

$$Y_{2,1}(t) = -\sqrt{\frac{15}{8\pi}} \cos\vartheta(t) \sin\vartheta(t)\, \mathrm{e}^{i\varphi(t)} \tag{7}$$

The Larmor angular frequency is given by $\omega = \gamma B_0$ where γ is the gyromagnetic ratio of the resonant nuclei and B_0 is the magnetic flux density the sample is subjected to in the magnet. C is a constant depending on the strength of the spin interactions. In the case of deuteron NMR, the intramolecular character of spin interactions is always warranted since coupling of the nuclear electric quadrupole moment with the electric field gradient in the molecule (or molecular group) dominates. On the other hand, the relaxation mechanism of protons is normally governed by dipole−dipole interactions which can be of an intra- or intermolecular nature. However, at least for frequencies $\nu > 10^6$ Hz, the intra contribution dominates by far for typical intramolecular proton−proton distances.[19]

From the empirical point of view, eq 6 suggests that any finite slope of the T_1 dispersion means that some finite correlation to the initial orientation of the molecule is still decaying on the time scale corresponding to the inverse Larmor angular frequency. For a more detailed description and explanations of the technique see ref 11.

The second method of primary interest is field-gradient NMR diffusometry directly reflecting the self-correlation function given in eq 3. In this case the wave vector is defined by

$$\mathbf{k} = \gamma\delta\mathbf{G} \tag{8}$$

δ is the spatial encoding time by the gradient $\boldsymbol{G}$ of the external magnetic field. Details of the method can be found in ref 15, for example.

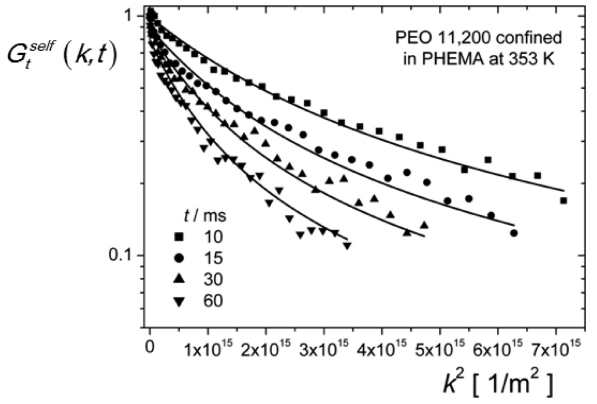

Figure 1. Self-correlation functions (eq 3) of a poly(ethylene oxide) melt, $M_w = 11\,200$, confined to PHEMA pores at 80 °C as a function of the squared wavenumber, k^2, for different diffusion times t (data from refs 21, 22). The data have been acquired with the aid of the field-gradient NMR diffusometry technique. Anticipating the tube/reptation model and using the formalism developed for this particular model[21,24] the data can be described by the solid lines commonly fitted to the data. The tube diameter as the only fitting parameter was found to be $a = (8 \pm 1)$ nm for this sample. This value coincides well with the pore diameter estimated from electron micrographs of the same sample. Other parameter values such as the number of statistical segments per chain $N = M_w/853$ and the segmental diffusivity $D_0 = 9.66 \times 10^{-10}$ m^2/s were taken from the literature for bulk melts.[25,26]

Results for the Self- and Pair-Correlation Functions under Nanometric Confinements

Figure 1 shows data of the self-correlation function, eq 3, measured with the field gradient NMR diffusometry technique as a function of the square wavenumber (see eq 8) in a system of poly(ethylene oxide) strands embedded in a rigid cross-linked polyhydroxyethyl methacrylate (PHEMA) matrix.[21,22] The curve parameter is the diffusion time. The preparation of the nanometric poly(ethylene oxide) (PEO) strands in this sample is based on spinodal decomposition and is described in detail in refs 20 and 21. The strand diameter was estimated with different methods including electron microscopy.[21−23] Modifying the preparation protocol, samples with diameters in a range from 8 up to 60 nm can be produced.[21]

The translational-diffusion results were shown to be compatible with the tube/reptation model[27] leading to the theoretical self-correlation function[21,24]

$$G_t^{self}(k,t) = \exp\left\{\frac{k^4 a^2 D_0 t}{36N}\right\} \operatorname{erfc}\left\{\frac{k^2 a\sqrt{D_0 t}}{6\sqrt{N}}\right\} \exp\left\{-\frac{\frac{2}{3}k^2 D_0 t}{N + 4D_0 t\left(\frac{2}{a}\right)^2}\right\} \quad (9)$$

(see eq 19 in ref 21). D_0 is the segmental diffusion coefficient based on the known segment friction coefficient. N is the number of Kuhn segments per chain. The values of these parameters are given in the legend of Figure 1. The dimension of the topological constraint, a, evaluated on this basis turned out to coincide with the real pore diameter determined with the aid of other techniques.[20,21] This means that no substantial confinement effect beyond restriction by the "pore" (or better "strand") walls can be stated for translational diffusion on the time scale of field-gradient NMR diffusometry experiments.

This result was later confirmed by incoherent neutron scattering applied to PEO confined in a solid matrix of anodic aluminum oxide.[28] This technique again probes the self-correlation function eq 3, but the time scale is intrinsically much shorter. Likewise, the (intramolecular) pair correlation function, eq 4, examined with the aid of coherent neutron scattering of deuterons located on the same macromolecule does not reveal any confinement effect of nanometrically confined polymer melts.[29,30] Note, however, that the quantitative parameter values specified in ref 29 on the one hand and in ref 30 on the other are incompatible with each other both in the bulk and confined PEO cases. Clarification of this discrepancy appears to be necessary before final conclusions can be drawn.

Results for Orientation Correlation Functions under Nanometric Confinements

The frequency dependence of the spin−lattice relaxation time T_1 is an efficient tool for probing the orientation correlation function eq 2 for $l = 2$ and $m = 1$ on the basis of eqs 6 and 7. As examples, parts a and b of Figure 2 show corresponding data of linear perdeuterated PEO melts measured under nanometric confinement in PHEMA and as bulk samples, respectively.[31] The dispersions of the deuteron spin−lattice relaxation time $T_1(\nu)$ are much steeper when confined in a solid matrix (Figure 2a) than in bulk (Figure 2b). The values of the spin−lattice and the transverse relaxation times as quantities reflecting the orientation correlation functions of segments are strongly reduced by up to 1 order of magnitude. This phenomenon was termed the corset effect: The orientation correlation function decays more slowly in confined polymers than in bulk. Segmental reorientation is more anisotropic under confinement than under bulk conditions. Rotational fluctuations are obviously more constrained under confinement than the translational displacements discussed in the previous section.

Remarkable and important features of the experiments represented by Figures 2a and b are as follows: (i) deuteron resonance selectively probes the perdeuterated PEO strands; (ii) deuteron spin−lattice relaxation is exclusively sensitive to rotational fluctuations of the quadrupolar spin interaction tensor, that is of the methylene segments of the polymer; (iii) the spin−lattice relaxation dispersion of the confined polymer approaches the power law $T_1 \propto M_w^0 \nu^{0.75}$, a feature of the tube/reptation model, at elevated frequencies in contrast to the bulk behavior (see ref 33); (iv) unlike proton spin−lattice relaxation there is no averaging mechanism effective in the case of deuterons, so that differences in the local spin−lattice relaxation rates due to different segment mobilities are not leveled.

Apart from these ^{2}H (deuteron) field-cycling NMR relaxometry studies, equivalent results have been found in numerous investigations based on ^{1}H (proton) and ^{19}F (fluorine) resonances.[34−38] In an extended series of experiments, the confining PHEMA matrices used for the experiments represented by Figure 2a have been modified to provide PEO strands with diameters varying from 8 to 60 nm with little effect on the corset effect.[34] Likewise, variation of the molecular mass of the polymer does not affect perceptibly the orientation correlation function under confinement whereas the bulk data undergo a transition from Rouse-like dynamics for $M_w < M_c$ to the so-called entangled behavior for $M_w > M_c$ where M_c is the critical molecular mass. This transition reveals itself by different orientation correlation functions qualitatively in the sense that entangled polymers retain their initial segment orientations much longer than freely draining chains.

In another series of experiments, perfluoropolyether (PFPE) has been confined in Vycor, a porous silica glass with a nominal pore diameter of 4 nm.[35,37] The ^{19}F spin−lattice relaxation dispersion again revealed a strong corset effect with a somewhat weaker dispersion slope. Furthermore, the same polymer confined as layers between Kapton foils wound to form rolls showed a small but

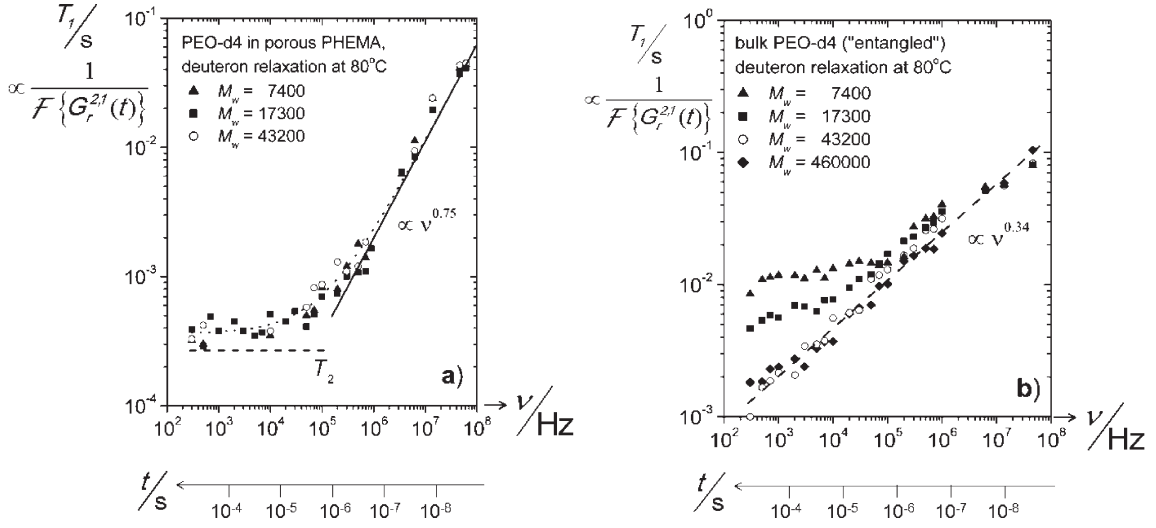

Figure 2. Examination of the orientation correlation function (eq 2 for $l = 2$, $m = 1$) via the frequency dependence of the deuteron spin−lattice relaxation time (see eq 6) of perdeuterated PEO confined in 10 nm pores of solid PHEMA at 80 °C (a) and in bulk melts (b) (data from ref31.). Different molecular masses M_w have been investigated. The dispersion of the confined polymers verifies the law $T_1 \propto M_w^0 \nu^{0.75}$ at high frequencies as predicted for limit $(II)_{DE}$ of the tube/reptation model.[32,33] The low-frequency plateau observed with the confined polymers indicates that the correlation function implies components decaying more slowly than the magnetization relaxation curves, so that the Bloch/Wangsness/Redfield relaxation theory[12] is no longer valid in this regime. This is confirmed by the fact that the plateau value corresponds to the transverse relaxation time, T_2, for deuterons extrapolated from the high-field value measured at 9.4 T. The spin−lattice relaxation dispersion $T_1 \propto M_w^0 \nu^{0.34}$ found for bulk melts in the limit of long polymer chains ($M_w \gg M_e$ where M_e is the critical molecular mass) represents the so-called "entangled dynamics" and can be reproduced with the aid of the renormalized Rouse formalism.[33] The time axes are defined by $t = 1/2\pi\nu$.

anyway clearly detectable retardation of the orientation correlation function relative to the bulk melt.[38]

Using again field-cycling NMR relaxometry, poly(ethylene oxide)/sodium montmorillonite nanocomposites have been examined in ref 39. The confinement dimension was about 1 nm. The samples contained bulk and confined polymer phases at the same time. The decomposition of the superimposed proton signals revealed a clear confinement effect up to about 1 order of magnitude. There are many more studies of layered confinement of polymers based on other NMR techniques. A review can be found in ref 1. The general tendency is that confinement leads to a more anisotropic character of segment reorientation so that the orientation correlation function decays more slowly at least as concerns its long-time tail.

More recently, polybutadiene confined in anodic aluminum oxide matrices (20 and 60 nm) and polydimethylsiloxane restrained to emulsion droplets (200−1000 nm) were studied with the aid of multiple-quantum build-up NMR spectroscopy.[8] Since the generation of multiple-quantum coherences requires finite residual dipolar spin couplings not averaged out by molecular motions on the NMR time scale, this technique is particularly sensitive to the anisotropy of the segment reorientations. This method probes the orientation correlation function eq 2 for $l = 2$ and $m = 0$, i.e.

$$G_r^{2,0}(t) = \langle Y_{2,0}(t) Y_{2,0}(0) \rangle \propto \langle P_2(t) P_2(0) \rangle \qquad (10)$$

where the second-order Legendre polynomials read

$$P_2(t) = \frac{1}{2} [3\cos^2 \vartheta(t) - 1]$$

Clear manifestations of the corset effect have been reported for all systems investigated in this study.

Confinement phenomena equivalent to the corset effect have also been found in dielectric relaxation studies. The complex dielectric constant $\varepsilon(\omega)$ for the angular frequency ω obeys[40]

$$\frac{\varepsilon(\omega) - \varepsilon(\infty)}{\varepsilon(0) - \varepsilon(\infty)} = -\int_0^\infty \exp\{i\omega t\} \dot{G}_P(t)\, \mathrm{d}t = 1 + i\omega L\{G_P(t)\} \qquad (11)$$

where

$$G_P(t) = \langle P(t) P(0) \rangle = \frac{\mu^2}{V^2} \sum_{l,m=1}^{N_d} \langle \cos \vartheta_l(t) \cos \vartheta_m(0) \rangle \qquad (12)$$

is the autocorrelation function of the macroscopic electric polarization $P(t)$, and $L\{...\}$ stands for the Laplace transfom. Equation 12 refers to a volume V containing N_d permanent electric dipoles. The angle ϑ_l is defined between the orientation of the $l-th$ dipole and the external electric field. Assuming a homogeneous, dilute distribution of the dipoles, so that cross-terms in eq 12 can be neglected and no position dependence exists, permits the approximation as a single-particle correlation function

$$G_P(t) \approx \frac{\mu^2 N_d}{V^2} \langle \cos \vartheta(t) \cos \vartheta(0) \rangle \qquad (13)$$

That is, in terms of eq 2, the orientation correlation function for $l = 1$ and $m = 0$ is probed:

$$G_r^{1,0}(t) = \langle Y_{1,0}(t) Y_{1,0}(0) \rangle \propto \langle \cos \vartheta(t) \cos \vartheta(0) \rangle \qquad (14)$$

Depending on the system under investigation, the approximation by a single-particle correlation function eq 14 may be problematic. However, even the macroscopic correlation function eq 12 already reflects dynamic reorientation properties so that dielectric relaxation spectroscopy is suitable for studies of rotational fluctuations in any case. On this basis, evidence for geometrical confinement effects on polymer chain dynamics independent of the chain length were reported in ref 13, Chapter 6, and ref 41. The systems examined were poly(propylene glycol) and poly(dimethylsiloxane) in nanoporous glasses. The interplay between adsorption and (geometrical) confinement effects was analyzed. Variation of the pore size permitted the clear identification of the geometrical confinement contribution.

Finally, in ref 9, a confinement effect in micrometer thick droplets was identified with the aid of mechanical relaxation in the sense of an increased terminal relaxation time. Mechanical relaxation cannot simply be traced back to single-particle correlation functions since it always refers to finite volume elements subjected

to deformations. However, any such shear deformation will be connected with reorientations of molecular entities so that the observed confinement effect can be considered to be analogous to the above examples.

Model Concepts

The corset effect manifests itself as a strong retardation of the long-time tail of the orientation correlation decay whereas translational fluctuations appear to be unaffected as far as can be concluded from the experiments described before. In other words, segmental reorientation is getting more anisotropic under confinement leaving a slowly decaying tail at times much longer than the relaxation times of short-range chain modes.

Of course, in a polymer melt translational and rotational fluctuations are not entirely independent of each other. Some correlation must be expected. Then it is a matter of the accessible ranges of the experimental parameters whether such a correlation reveals itself in methods probing translational displacements. The time and length scales of neutron scattering and field-gradient NMR diffusometry, for instance, are very different. While the incoherent neutron scattering technique used in ref 28 probes a time scale $t \leq 10^{-10}$ s and a length scale 8.3×10^{-11} m $\leq k^{-1} \leq 5 \times 10^{-10}$ m, the field-gradient NMR diffusometry method employed in ref 21 is characterized by typical ranges $t \geq 10^{-2}$ s and $k^{-1} \geq 12.5$ nm. The respective limits of detectable root-mean-square particle displacements are $\langle r^2(t)\rangle^{1/2} < 0.7$ nm and $\langle r^2(t)\rangle^{1/2} > 10$ nm for incoherent neutron scattering and field-gradient NMR diffusometry.

As will be seen below, the theories describing the corset effect predict a confinement dimension just in between so that both techniques are not expected to be sensitive to the aforementioned correlation. Note, however, that the relatively long time and length scales intrinsic to field-gradient NMR diffusometry imply the scales on which the corset effect reveals itself. The NMR diffusometry decay curves (such as the ones shown in Figure 1) have been described by the tube/reptation model with the electron microscopically determined pore diameter as the "tube" diameter and bulk values for all other parameters. This suggests that any influence of translation/rotation correlations must be minor.

The corset effect can be interpreted on different levels. The simplest conclusion one can draw from the different slopes of the T_1 dispersion in bulk and under confinement is a different degree of anisotropy of molecular dynamics. The steeper dispersion slope and the reduced transverse relaxation times under confinement mean that the long-time decay of the correlation function eq 2 is retarded relative to the bulk sample. Segmental isotropization so-to-speak takes longer. The origin of this retardation can only be a stronger influence of topological constraints hindering rotational rearrangements of chain sections. The corset effect can therefore be traced back to topological constraints that are more efficient for conformational fluctuations.

On the next level, one can identify the corset effect as a finite-size phenomenon.[43] A well-known law of statistical physics relates the mean square fluctuation of the particle number in a given volume to the mean number of particles in that volume:

$$\langle (\delta N_V)^2 \rangle = k_B T \rho_s \kappa_T \langle N_V \rangle \tag{15}$$

k_B is Boltzmann's constant, T is the absolute temperature, ρ_s is the mean (segment) particle number density, κ_T is the isothermal compressibility of the system. That is, fluctuations in large systems are larger than in small system. Reducing the system size by confinement consequently reduces the fluctuations. In terms of the fluctuating free volume, this means that conformational fluctuations are also restricted in their extent. The corresponding topological constraints are stronger. A scaling treatment in refs 34 and 43 suggest a dimension of those constraints in the order of

$$d \approx \sqrt{b^2 \rho_s k_B T \kappa_T} \tag{16}$$

where b is the root-mean-square end-to-end distance of a statistical segment. Although eq 16 has the character of a rough estimation, it gives an idea what dimension can be expected for topological constraints under confinement.

On the same basis, bulk behavior was predicted for the limit

$$d_{pore} \gg \left(\frac{b^3}{k_B T \kappa_T} \right)^{1/3} R_F \tag{17}$$

where R_F is the Flory radius of a bulk polymer random coil. Inserting typical values for the parameters in eq 16 leads to values in the order of nanometers for the topological constraints causing the corset effect. Likewise eq 17 suggests a crossover to bulk behavior on a pore dimension scale in the order of micrometers. Actually, a small but anyway finite effect has indeed observed on this confinement length scale.[38]

The third level of interpretation refers to the Doi/Edwards model for reptation in a fictitious tube.[27] Identifying the extension of the relevant topological constraints with the fictitious Doi/Edwards tube unavoidably leads to a very tight diameter if the strong anisotropy of rotational fluctuations is to be explained: In the frame of this model, the tube is the only source of anisotropy apart from chain connectivity.

We note that the power law

$$T_1 \propto M_w^0 \nu^{0.75} \tag{18}$$

appearing in Figure 2a in the upper half of the frequency window coincides with the prediction for the characteristic limit $(II)_{DE}$ of the tube/reptation model for a time scale between the so-called entanglement time and the longest Rouse relaxation time.[33] Interestingly the tube diameter derived from the experimental data on the basis of the tube/reptation model fits to the value estimated on the basis of eq 16 when this expression is taken to represent the extension of the tube. As argued above, the conclusion suggested by this interpretation is valid specifically for rotational fluctuations. On the other hand, translational fluctuations as revealed by field-gradient NMR diffusometry and neutron scattering are obviously not very sensitive to this feature of molecular dynamics.

By the way, the condition for which de Gennes originally derived his reptation expression[42] for the dynamic structure factor is $ka \ll 1$, where a is the tube diameter. The value usually considered to be relevant for bulk polymer melts is $a \approx 5$ nm, so that the limit $k \ll 0.2$ nm^{-1} should be reached in experiments supposed to probe the tube. In reality, however, only wavenumber values $k > 0.2$ nm^{-1} can be reached for technical reasons. The interpretation of corresponding data therefore needs reconsideration on the basis of a rigorous theory with an extended range of applicability. Unfortunately, this is not yet available.

Finally, the role of surface adsorption as a potential origin of phenomena with a similar appearance as the corset effect should be considered. This is of a quite important issue that must be discussed for the specific polymer/matrix system examined in the References referred to above. Let us now give five arguments how perceptibly surface adsorption can be identified, distinguished or ruled out for the systems for which the corset effect was measured in refs 34, 35, and 37.

(i) From the experimental point of view, the existence of adsorbed, i.e., immobilized, phases would have revealed themselves as distinct relaxation or diffusion components (as it was actually observed in the polydimethylsiloxane/Vycor system studied in ref 44). This is not the case in the PHEMA samples and

in the other systems for which a corset effect was identified, neither with field-cycling NMR relaxometry and transverse relaxation nor with field-gradient NMR diffusometry. As concerns spin−lattice relaxation, it should be recalled in this context that immaterial spin diffusion by flip-flop transitions as an averaging mechanism is not effective for deuterons. (ii) The PEO strands in methacrylate matrices were prepared on the basis of spinodal decomposition.[21,20] That is, the polymers under study were so-to-speak expelled from the matrix material, and softly repulsive polymer/wall interactions are expected. Likewise, the fluorine containing polymer studied in ref 35 is a compound with little affinity to the surfaces of the matrix material. (iii) In the case of the methacrylate samples, the PEO strand diameters and, hence, the surface to volume ratio were varied in a wide range with almost no effect on the results.[34] (iv) The corset effect vanishes when frequency/time scales are approached where short-range chain modes, so-called "local motions", dominate. (v) Chemical surface modification will alter adsorption affinities in contrast to the geometrical confinement effect. In this way, the two phenomena have unambiguously been distinguished and identified in ref 41.

Conclusions

Diverse dynamical methods suitable for probing polymer chain dynamics have been considered. In order to be able to compare results on a common basis independent of method specific terms, the discussion is based on correlation functions specific for certain types of fluctuations but not for the techniques themselves. We thus distinguish correlation functions of the dynamic-structure-factor type probing absolute or relative particle displacements from autocorrelation functions of spherical harmonics of different orders depending on molecular (or segmental) reorientations. Typical methods to be attributed to these two categories are field-gradient NMR diffusometry and quasi-elastic neutron scattering on the one hand, and field-cycling NMR relaxometry, dielectric relaxation, multiple-quantum build-up NMR spectroscopy, and mechanical relaxation on the other.

On the basis of the results obtained with the various techniques, it turns out that translational and rotational fluctuations are subject to substantially different topological constraints when confined in nanometric matrices. Methods probing translational fluctuations such as field-gradient NMR diffusometry and neutron scattering do not reveal any significant confinement effect in contrast to all techniques sensitive to orientation correlation functions. The latter are sensitive to topological constraints obviously more efficient than those acting on translational fluctuations.

In the particular systems studied in refs 34, 35, and 37, no perceptible manifestation of surface adsorption was found. On the other hand, adsorption phenomena have been identified as a separate and independent mechanism in refs 13, 41, and 44 based on NMR spin−lattice relaxation and broadband dielectric spectroscopy. The corset effect, i.e. the confinement effect based on the topological constraints specifically acting on rotational fluctuations, can be explained on a geometrical basis as a finite- size confinement phenomenon. An interpretation of the constraints in terms of the Doi/Edwards tube is also possible. However, the tube diameters estimated on this basis from data sets obtained with the two categories of techniques strongly deviate from each other. Obviously, the tube/reptation model in general and the description of topological constraints in terms of a tube in particular are not specific enough to account for translational and rotational segment dynamics at the same time.

Acknowledgment. Financial support by RFBR (Grant No. 8470; 10-03-00739-a) and the DAAD is gratefully acknowledged.

References and Notes

(1) Giannelis, E. P.; Krishnamoorti, R.; Manias, E. *Adv. Polym. Sci.* **1999**, *138*, 107–147.
(2) Schönhals, A.; Rittig, F.; Kärger, J. *J. Chem. Phys.* **2010**, *133*, 094903.
(3) Kim, T.-S.; Mackie, K.; Zhong, Q.; Peterson, M.; Konno, T.; Dauskardt, R. H. *Nano Lett.* **2009**, *9*, 2427–2432.
(4) Ayalur-Karunakaran, S.; Blümich, B.; Stapf, S. *Eur. Phys. J. E: Soft Matter Biol. Phys.* **2007**, *26*, 43–53.
(5) Gu, H.; Faucher, S.; Zhu, S. *AIChE J.* **2010**, *56*, 1684–1692.
(6) Buntkowsky, G.; Breitzke, H.; Adamczyk, A.; Roelofs, F.; Emmler, T.; Gedat, E.; Gruenberg, B.; Xu, Y.; Limbach, H.-H.; Shenderovich, I.; Vyalikhz, A.; Findenegg, G. *Phys. Chem. Chem. Phys.* **2007**, *9*, 4843–4853.
(7) Valiullin, R.; Kärger, J.; Gläser, R. *Phys. Chem. Chem. Phys.* **2009**, *11*, 2833–2853.
(8) Ok, S.; Steinhart, M.; Serbescu, A.; Franz, C.; Chavez, F. V.; Saalwächter, K. *Macromolecules* **2010**, *43*, 4429–4434.
(9) Liu, C.-Y.; Zhang, B.; He, J.; Keunings, R.; Bailly, C. *Macromolecules* **2009**, *42*, 7982–7985.
(10) Berne, B. J.; Pecora, R., *Dynamic Light Scattering*: Wiley: New York, 1976; Chapter 11.
(11) Kimmich, R.; Anoardo, E. *Prog. NMR Spectrosc.* **2004**, *44*, 257–320.
(12) Kimmich, R. *NMR Tomography, Diffusometry, Relaxometry*; Springer: Berlin, 1997.
(13) Kremer, F.; Schönhals, A., *Broadband Dielectric Spectroscopy*; Springer: New York, 2003.
(14) Kivelson, D.; Madden, P. *Mol. Phys.* **1975**, *30*, 1749–1780.
(15) Ardelean, I.; Kimmich, R. *Annu. Rep. NMR Spectrosc.* **2003**, *49*, 43–115.
(16) Fleischer, G.; Fujara, F. In *NMR—Basic Principles and Progress, Solid State NMR*; Diehl, P., Fluck, E., Günther, H., Kosfeld, R., Seelig, J., Eds.; Springer: Berlin, 1994, Vol. *30*, pp 159−207.
(17) Richter, D.; Monkenbusch, M.; Arbe, A.; Comenero, J. *Adv. Polym. Sci.* **2005**, *174*, 1–221.
(18) Kehr, M.; Fatkullin, N.; Kimmich, R. *J. Chem. Phys.* **2007**, *126*, 094903−1–094903−8.
(19) Kehr, M.; Fatkullin, N.; Kimmich, R. *J. Chem. Phys.* **2007**, *127*, 084911−1–084911−7.
(20) Beginn, U.; Fischer, E.; Pieper, T.; Mellinger, F.; Kimmich, R.; Möller, M. *J. Polym. Sci. A: Polym. Chem.* **2000**, *38*, 2041–2056.
(21) Fischer, E.; Beginn, U.; Fatkullin, N.; Kimmich, R. *Macromolecules* **2004**, *37*, 3277–3286.
(22) Fischer, E.; Kimmich, R.; Beginn, U.; Möller, M.; Fatkullin, N. *Phys. Rev. E* **1999**, *59*, 4079–4084.
(23) Fischer, E.; Beginn, U.; Fatkullin, N.; Kimmich, R. *Magn. Reson. Imaging* **2005**, *23*, 379–381.
(24) Fatkullin, N.; Kimmich, R. *Phys. Rev. E* **1995**, *52*, 3273–3276.
(25) Smith, G. D.; Yoon, D. Y.; Jaffe, R. L.; Colby, R. H.; Krishnamoorti, R.; Fetters, L. J. *Macromolecules* **1996**, *29*, 3462–3469.
(26) Graessley, W. W.; Edwards, S. F. *Polymer* **1981**, *22*, 1329–1334.
(27) Doi, M.; Edwards, S. F. *The Theory of Polymer Dynamics*; Oxford Univ. Press: Oxford. U.K., 1986.
(28) Kroutyeva, M.; Martin, J.; Arbe, A.; Colmenero, J.; Mijangos, C.; Schneider, G. J.; Unruh, T.; Su, Y.; Richter, D. *J. Chem. Phys.* **2009**, *131*, 174901−1–174901−11.
(29) Martin, J.; Krutyeva, M.; Monkenbusch, M.; Arbe, A.; Allgaier, J.; Radulescu, A.; Falus, P.; Maiz, J.; Mijangos, C.; Colmenero, J.; Richter, D. *Phys. Rev. Lett.* **2010**, *104*, 197801−1–197801−4.
(30) Lagrené, K.; Zanotti, J.-M.; Daoud, M.; Farago, B.; Judeinstein, P. *Phys. Rev. E* **2010**, *81*, 060801−1–060801−4.
(31) Kimmich, R.; Seitter, R.-O.; Beginn, U.; Möller, M.; Fatkullin, N. *Chem. Phys. Lett.* **1999**, *307*, 147–152.
(32) de Gennes, P. G. *J. Chem. Phys.* **1971**, *55*, 572–580.
(33) Kimmich, R.; Fatkullin, N. *Adv. Polym. Sci.* **2004**, *170*, 1–113.
(34) Mattea, C.; Fatkullin, N.; Fischer, E.; Beginn, U.; Anoardo, E.; Kroutieva, M.; Kimmich, R. *Appl. Magn. Reson.* **2004**, *27*, 371–381.
(35) Kausik, R.; Mattea, C.; Kimmich, R.; Fatkullin, N. *Eur. Phys. J. Spec. Top.* **2007**, *141*, 235–241.
(36) Fatkullin, N.; Kausik, R.; Kimmich, R. *J. Chem. Phys.* **2007**, *126*, 094904−1–094904−8.
(37) Kausik, R.; Fatkullin, N.; Hüsing, N.; Kimmich, R. *Magn. Reson. Imaging* **2007**, *25*, 489–492.
(38) Kausik, R.; Mattea, C.; Fatkullin, N.; Kimmich, R. *J. Chem. Phys.* **2006**, *124*, 114903−1–114903−5.

(39) Krzaczkowska, J.; Strankowski, M.; Jurga, S.; Jurga, K.; Pietraszko, A. *J. Non-Cryst. Solids* **2010**, *356*, 945–951.
(40) Glarum, S. H. *J. Chem. Phys.* **1960**, *33*, 1371–1375.
(41) Schönhals, A.; Goering, H.; Schick, Ch. *J. Non-Cryst. Solids* **2002**, *305*, 140–149.
(42) de Gennes, P. G. *J. Phys.* (*Paris*) **1981**, *42*, 735–740.
(43) Fatkullin, N.; Kimmich, R.; Fischer, E.; Mattea, C.; Beginn, U.; Kroutieva, M. *New J. Phys.* **2004**, *6*, 46–1 − 46−13.
(44) Stapf, S.; Kimmich, R. *Macromolecules* **1996**, *29*, 1638–1641.